

Article

Residential Buildings' Real Estate Values Linked to Summer Surface Thermal Anomaly Patterns and Urban Features: A Florence (Italy) Case Study

Giulia Guerri ¹, Alfonso Crisci ¹, Irene Cresci ², Luca Congedo ³, Michele Munafò ³ and Marco Morabito ^{1,4,*}

¹ Institute of Bioeconomy (IBE), National Research Council, 50019 Florence, Italy; giulia.guerri@ibe.cnr.it (G.G.); alfonso.crisci@ibe.cnr.it (A.C.)

² MSc Environmental Sciences, Wageningen University and Research, Droevendaalsesteeg 4, 6708 PB Wageningen, The Netherlands; irene.cresci@wur.nl

³ Italian National Institute for Environmental Protection and Research (ISPRA), 00144 Rome, Italy; luca.congedo@isprambiente.it (L.C.); michele.munafò@isprambiente.it (M.M.)

⁴ Centre of Bioclimatology (CIBIC), University of Florence, 50144 Florence, Italy

* Correspondence: marco.morabito@cnr.it; Tel.: +39-055-5226041

Citation: Guerri, G.; Crisci, A.; Cresci, I.; Congedo, L.; Munafò, M.; Morabito, M. Residential Buildings' Real Estate Values Linked to Summer Surface Thermal Anomaly Patterns and Urban Features: A Florence (Italy) Case Study. *Sustainability* **2022**, *14*, 8412. <https://doi.org/10.3390/su14148412>

Academic Editors:
Carmelo Maria Torre,
Alessandro Bonifazi
and Maria Cerreta

Received: 8 June 2022

Accepted: 6 July 2022

Published: 8 July 2022

Publisher's Note: MDPI stays neutral with regard to jurisdictional claims in published maps and institutional affiliations.



Copyright: © 2022 by the authors. Licensee MDPI, Basel, Switzerland. This article is an open access article distributed under the terms and conditions of the Creative Commons Attribution (CC BY) license (<https://creativecommons.org/licenses/by/4.0/>).

Abstract: Climate-change-related extreme events impact ecosystems, people, economy, and infrastructures, with important consequences on the real estate market as well. This study aims to investigate the variation of residential buildings' real estate values in a historic Italian city in relation to the summer surface thermal anomaly pattern and urban features surrounding buildings. Open data from remote sensing products and the national database of the Revenue Agency of Italy were used. Real estate values of residential buildings were spatially analyzed in four urban belts, and the association with daytime summer surface hot- and cool-spot zones was studied through odds ratio (OR) statistic. Urban features (impervious area, tree cover, grassland area, and water body) surrounding residential buildings with different real estate values were also analyzed. Considering the whole Florentine municipality, 13.0% of residential buildings fell into hot-spot zones (only 0.6% into cool-spot ones), characterized by very low tree cover surfaces (generally <1%), most of which were in the central belt (37% of all buildings in central belt). Almost 10% of these buildings belonged to the highest market value class revealing a positive association (OR = 1.53) with hot-spot zones. This study provides useful information to plan targeted building interventions to avoid a probable decrease of the value of residential properties in high heat-related risk areas.

Keywords: real estate market; surface thermal anomalies; urban features; remote sensing; thermal hot-spot.

1. Introduction

There is abundant scientific literature demonstrating the devastating effects in general on ecosystems, people, economy, and infrastructures caused by the increase in global temperature, with future projections that could sadly be even worse [1,2]. Important repercussions are currently being experienced or expected in the near future in most densely populated urban areas where the thermal effect is amplified by the anthropogenic phenomenon known as urban heat island (UHI) [3–6]. Unvegetated and larger paved areas contribute to create “micro-urban heat islands” which seriously complicate local livability [7–9]. The situation is also particularly critical in some European cities that in recent years have seen a significant increase in extreme weather events (such as destructive storms, strong winds, heavy precipitation, etc.) and especially the frequency and intensity of heat waves [10–12].

Among the many heat-related effects that we are unfortunately already experiencing (impacting the human health, energy consumption, and water demand, to name a few), others will have an effect in the medium- to long-term. From the beginning of the 21st century, much attention has been paid to the impact on the real estate price of some climate-change-related extreme events, such as destructive storms, sea level rise, floods, and wildfires [13–18]. However, very little has been addressed regarding the potential effect of intra-urban thermal anomalies on the residential housing market [19], representing an emerging problem with potential impacts on local economies.

Urban surface thermal anomalies depend on the trade-off between certain urban elements, such as the amount of impervious areas and blue and green infrastructures, in addition to morphological features [20]. This situation can locally create new cooling needs for buildings' indoor environments, significantly increasing operations costs at real estate assets. Extreme heat can also affect consumer behavior, and in the long-term, it could have indirect effects on the residential real estate market as consumer preferences shift. This aspect is of relevance especially in Europe, which is considered as one of the most attractive regions worldwide for investments in real estate.

At the Italian level, more than 70% of the population are homeowners (<https://www.statista.com/topics/6777/residential-real-estate-in-italy/>, accessed on 7 June 2022) and the residential sector is the largest in the real estate market. Since houses or flats are generally considered an important and safe investment, studies aimed at evaluating how rising temperatures impact residential real estate increasingly represent an emerging need.

This study aims to investigate the variation of residential buildings' real estate value in the municipal area of Florence (Tuscany, Italy) in relation to the summer intra-urban surface thermal pattern [20,21], also accounting for the contribution of urban infrastructures (such as the presence of grassy and arboreal surfaces, land consumption, and water bodies) surrounding (considering different buffer areas) residential buildings. The surface thermal pattern layer is represented by clusters of hot- and cool-spot zones obtained by applying a robust statistical spatial method based on the summer land surface temperature layer (Landsat-8 remote sensing data).

The research hypothesis of this study is to quantitatively verify that the increase in the real estate value of residential buildings is associated with favorable surface thermal patterns (the possibility that a residential building is located out from a hot-spot zone) and a greater concentration of green-blue infrastructures in the proximity of residential buildings.

2. Materials and Methods

2.1. Study-Area

This study was carried out in Florence (Tuscany, central Italy), a municipality with an average elevation of about 50 m, an extension of 100 km² and about 400,000 inhabitants. This city was selected because it has the largest historical, cultural, and landscape heritage among Italian municipalities.

According to the Köppen–Geiger climate classification [22], the municipal area of Florence has a borderline Mediterranean (Csa) and Humid subtropical climate (Cfa), with a moderate influence of the sea and warm summers. July and August represent the warmest months in all cities investigated, whereas the coldest months are December and January (source: Environmental Modeling and Monitoring Laboratory for Sustainable Development, LaMMA Consortium, <http://www.lamma.rete.toscana.it/en/node/13782>, accessed on 7 June 2022). In the summer period, the average and maximum monthly temperatures are 22.0 °C and 28.3 °C in June, and about 25.0 °C and 32.0 °C in July and August. In the winter period, the average and minimum monthly temperatures are 7.1 °C and 3.2 °C in December, 6.4 °C and 2.2 °C in January, and 7.3 °C and 2.5 °C in February.

Data from the Italian National Institute of Environmental Protection and Research (ISPRA) [23] showed a high degree of imperviousness with 41.7% soil consumption (4267 ha)

in Florence in 2019, showing one of the highest growths in artificial surfaces among Italian regional capitals.

2.2. Study Framework and Methodological Approach

In this study, open data sourced from: (i) remote sensing products (Landsat-8 and Copernicus Sentinel-2 missions); (ii) the national demographic (Italian National Institute of Statistics); and (iii) real estate value databases (Real Estate Market Observatory of the National Revenue Agency of Italy) were used to perform spatial-statistical analyses in open QGIS [24] and IBM SPSS (IBM Statistical Package for Social Science) [25] environments. In particular, remote sensing data from Landsat-8 imageries were used for the daytime summer Land Surface Temperature (LST) calculation, with the aim to study surface thermal extremes, which are globally more pronounced when the sun is shining during daytime and in the summer period [26–28]. Sentinel-2 imageries at 10 m horizontal resolution were used for obtaining the urban features layers (surface albedo, tree cover, grassland, and impervious area). Residential buildings data were spatially extracted by using the buildings database of the Tuscany Region (GEOscopio platform, <http://www502.regione.toscana.it/geoscopio/cartoteca.html>, accessed on 7 June 2022).

Some residential buildings and surrounding (considering a perimetric buffer area of 50 m and 100 m) building characteristics were analyzed in the municipal area of Florence classified by the Italian official organization that investigates and describes the market value of real estate.

The study framework was developed following two main phases:

- Descriptive analyses concerning the characterization of residential buildings located in different urban areas based on the number, density, and dimension (area and volume) of residential building units, as well as including demographic (resident population and population density), surface (the average albedo and land surface temperature of residential building's roofs), and morphological (Sky View Factor surrounding residential buildings) data.
- Investigation of the relationships between residential buildings' real estate values, surface thermal anomaly patterns, and urban green, blue, and grey infrastructures surrounding residential buildings, by considering two buffer areas with different sizes (50 m and 100 m). The buffer area was calculated following a homogeneous criterion starting from the perimeter of each residential building unit, with the aim of considering the surrounding characteristics proximal to residential buildings. Residential buildings falling into summer thermal hot- and cool-spot zones were investigated and compared with buildings falling in those thermally neutral.

2.3. Residential Buildings Real Estate Values

Residential buildings' real estate values from 2020 were available for specific urban areas of the Florence municipality and were obtained from the Real Estate Market Observatory (OMI) of the National Revenue Agency of Italy. OMI is the Italian national observatory that provides the real estate quotations related to residential, commercial, tertiary, and productive properties, expressed as a range of values (minimum and maximum values) per unit of area in euro per square meter (source: <https://www1.agenziaentrate.gov.it/servizi/Consultazione/ricerca.htm>, accessed on 7 June 2022).

The primary OMI classification was based on the subdivision of the Florentine municipal territory into four urban areas classes, named "OMI belts" [29]: central, semi-central, peripheral, and suburban areas. The central belt was the municipal portion coinciding with the urban center, intended as distinguishable building aggregate perimeter, able to exert attraction toward a larger settlement. The semi-central belt was in an intermediate position between the central and the peripheral belts, directly connected to the urban center by services, transports, and infrastructures. The peripheral belt was

contiguous to the semi-central one and was delimited by the outer margin of the built-up settlement, whereas the suburban one contained urbanized areas separated from the main urban agglomeration by undeveloped areas, natural, or artificial barriers.

Each OMI belt includes a variable aggregation of contiguous and homogeneous territorial areas, named “OMI zones”, each characterized by a specific residential building real estate value. These latter zones revealed uniformity of appreciation for economic and socio-environmental conditions [29]. This uniformity was translated into homogeneity in positional, historical-environmental, and socio-economic characteristics of settlements, provision of services, and urban infrastructure.

The basic information collected for the formation of each OMI zone were the following: prevailing destination, state and type, year of building construction, average number of floors, average surface of the real estate units, presence of public services, commercial, public green, level of the transport services, parking and road connections, commercial vocation, zone quality, and presence of historical sites.

2.4. Characterization of Residential Buildings Located in Different OMI Belts

Residential buildings located in specific OMI belts of the Florence municipality were characterized based on the average number, density, and dimensions of the residential building units, and on the demographic, surface, and morphological features:

- Number, density, surface areas, and volumes of the residential building units from the 2011 census were extracted by the buildings database of the Tuscany Region (GEOscopio platform) by filtering the residential building category class;
- Resident population and population density data were provided by the Italian National Institute of Statistics (ISTAT, <https://www.istat.it/en/>, accessed on 7 June 2022), through the regional database of Tuscany (GEOscopio platform), referring to the year 2011;
- Land Surface Temperature (LST) of residential building roofs was obtained by using Landsat 8 TIRS (Thermal Infrared Sensor) remote sensing data resampled to 30 m horizontal resolution (the original resolution of TIRS bands was 100 m) by the U. S. Geological Survey (<https://earthexplorer.usgs.gov/>, accessed on 7 June 2022). LST was retrieved for clear-sky days (cloud cover < 5%) selected from June to August of the 2015–2019 daytime (09:58 UTC) summer period (June-July-August). Mean summer daytime LST was calculated by using all available images converted from Kelvin to Celsius degrees (°C) by the following method developed by the U.S. Geological Survey and also applied in previous studies on the same study-area [20,21] (Equations (1) and (2)):

$$LST = T_b / [1 + (\lambda \cdot T_b / c^2) \cdot \ln(\epsilon)] \quad (1)$$

where λ is the wavelength of emitted radiance (10.8 μm); and c^2 is obtained by the following Equation (2):

$$c^2 = h \cdot c / s = 14,388 \mu\text{m K} \quad (2)$$

where h is the Planck’s constant (6.626×10^{-34} J s); c is the speed of light (2.998×10^8 m/s); and s is the Boltzmann constant (1.38×10^{-23} J K⁻¹).

- Surface albedo of residential building roofs was obtained by using Sentinel-2 Level 2A remote sensing product (10 m horizontal resolution) of the Copernicus mission (<https://scihub.copernicus.eu/dhus/#/home>, accessed on 7 June 2022), which referred to the 2017 daytime (from 10:00 to 11:00 UTC) summer period (from July to August), according to the method developed by a recent study [30]. The following Equations (3) and (4) were used to retrieve the surface broadband albedo (α) by considering the observed surface as Lambertian [30]:

$$\alpha = \sum_{B=1}^N p_B \cdot w_B \quad (3)$$

$$w_B = \frac{\int_{L_B}^{H_B} R_{s\lambda} \cdot d\lambda}{\int_{0.3}^3 R_{s\lambda} \cdot d\lambda} \quad (4)$$

where p_B is the surface reflectance for a specific band B ; w_B is the weighting coefficient; $R_{s\lambda}$ is the extraterrestrial solar radiation for the wavelength; $d\lambda$ is the bandwidth; L_B and H_B are the lowest and the highest wavelength limits assigned to Sentinel-2 bands. These equations were applied on the VNIR (B2, B3, B4 and B8) and SWIR (B11 and B12) bands.

- Sky View Factor (SVF) was obtained by the Digital Surface Model (1 m horizontal resolution, year 2017) in the QGIS environment by using 100 m radius and 16 search directions, as indicated in previous studies evaluating urban environments [31–33]. As suggested by previous studies, a 100 m radius was considered the best and most useful search area for urban studies. SVF values were averaged on each OMI belt with the aim to evaluate the urban morphology. The retrieval formula (Equation (5)) was used by considering the height of the obstacle (H) and the distance between obstacles (W) [34]:

$$SVF = \cos(\tan^{-1}(2 \cdot H/W)) \quad (5)$$

Further details on LST, albedo, and SVF retrieval methods were described in previous studies [20,21].

2.5. Focus on Surface Thermal Anomaly Patterns and Urban Features

In this study, the daytime summer LST layer was used to perform the intra-urban surface thermal anomaly cluster detection. The surface thermal anomaly pattern was obtained by adopting the Getis-Ord G_i^* statistical-spatial approach [35], already used in previous studies carried out on the Florentine metropolitan area [20], by performing a readjustment analysis only considering the Florence municipal area. The final surface thermal anomaly cluster layer spatially identified hot- and cool-spot zones, where high and low LST clusters were respectively distributed.

The number of residential buildings for each OMI belt (central, semi-central, peripheral, and suburban belts) falling into hot- and cool-spot zones was extracted according to four OMI zone classes (OMI_C): ranging from OMI_C1 to OMI_C4 with the lowest and highest residential building real estate values, respectively. These four OMI zones corresponded to residential building real estate value quartiles when enough real estate values were available within a specific OMI belt. Preliminarily and for each OMI belt, we investigated the existence of a possible relationship between LST, urban features (green, blue and grey infrastructures), and OMI_C through linear regression analyses. For these purposes, the relative R-squared and the associated statistically significant level (p value) were shown.

Odds ratios (OR) for residential buildings falling into hot- and cool-spot zones (exposure) and the associated real estate value classes (outcome) were also calculated by using a two-by-two contingency table in SPSS environment [25].

For this purpose and for each OMI belt, the following variables were selected, and this working scheme was followed:

- a = buildings in hot-spot (or cool-spot) zones belonging to a specific OMI class (therefore OMI_C1, OMI_C2, OMI_C3 or OMI_C4);
- b = buildings in hot-spot (or cool-spot) zones belonging to other OMI classes;
- c = buildings in non-hot-spot (or cool-spot) zones belonging to a specific OMI class;
- d = buildings in non-hot-spot (or cool-spot) zones belonging to other OMI classes.

The OR was calculated as (Equation (6)):

$$OR = \frac{a/c}{b/d} \quad (6)$$

Hence, the OR was applied to evaluate the probability that residential buildings with a specific market value (focused group) fall into surface thermal hot- or cool-spot zones, compared to buildings with other market values (control group). An OR value higher (or lower) than 1.0 revealed that the probability of being into a hot-/cool-spot zone is higher (or lower) in the focused group than the control group, and there is a positive association when $OR > 1$ and a negative association when $OR < 1$. On the other hand, an OR equal to 1 means equal probability of being into a hot-/cool-spot zone for both focused and control groups (no association between the exposure and the outcome).

Furthermore, each residential building was characterized based on the surrounding urban features (considering a buffer area of 50 m and 100 m) by using QGIS functions. In addition to the LST surrounding residential buildings, the following urban green, blue, and grey infrastructures layers (binary raster data) obtained from remote sensing data (10 m horizontal resolutions) of the Copernicus mission, the Italian National Institute for Environmental Protection and Research (ISPRA), and regional database of Tuscany were selected:

- green infrastructures, such as tree cover (TC), and grassland area (GA);
- blue infrastructure, such as water bodies (WB);
- grey infrastructure, such as impervious area (IA).

Green and grey infrastructures layers were based on a methodology developed by ISPRA and referred to the Copernicus Programme, also using different thresholds of the Normalized Difference Vegetation Index (NDVI) layer. Further details were reported in several national studies [36–40]. Water bodies data (including rivers, ponds, wetlands, and any other open water) were obtained from the Regional Land Cover Map, produced by the Environmental Modelling and Monitoring Laboratory for Sustainable Development, LaMMA Consortium (<http://www.lamma.rete.toscana.it/>, accessed on 7 June 2022).

The selected urban features were quantitatively calculated and averaged for each buffer area surrounding buildings belonging to a specific real estate value class (OMI_C), as shown in Figure 1. The average variations of urban features surrounding residential buildings among the four OMI_C were investigated by using the non-parametric Mann–Whitney [41] and Kruskal–Wallis [42] tests in IBM SPSS Statistics environment [23].

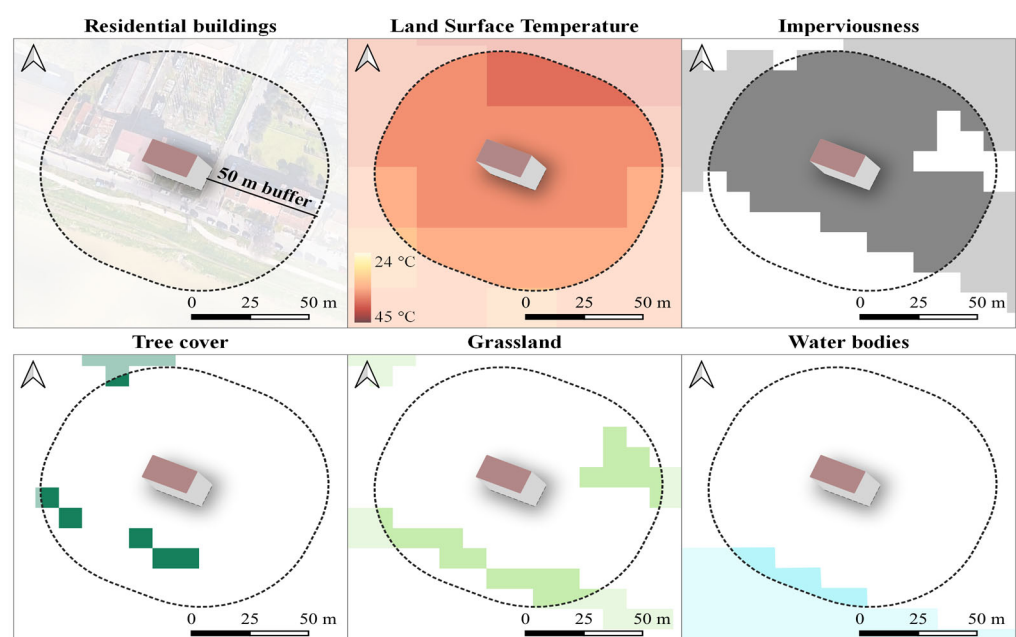


Figure 1. The selected urban features within the buffer area of 50 m surrounding residential buildings: land surface temperature (LST), imperviousness, tree cover, grassland, and water bodies.

3. Results

3.1. Descriptive Analyses

The OMI urban belt characterized by the largest surface area was the peripheral belt (representing 52% of the whole Florentine municipality), followed by the semi-central (35.8%), central (7.2%), and suburban (5.0%) ones.

The descriptive analyses regarding residential buildings and population, surface and morphological features in each OMI belt were shown in Table 1.

Table 1. Descriptive analyses on residential buildings, population, surface, and morphological features in each OMI belt.

Belt Features	Central Belt	Semi-Central Belt	Peripheral Belt	Suburban Belt
Belt area km ² (%)	7.4 (7.2)	36.6 (35.8)	53.3 (52.0)	5.1 (5.0)
Residential building N. (%)	19,715 (26.6)	31,601 (42.6)	21,398 (28.9)	1426 (1.9)
Residential building area m ² (%)	2.7 × 10 ⁶ (27.5)	3.9 × 10 ⁶ (40.8)	2.9 × 10 ⁶ (30.3)	0.1 × 10 ⁶ (1.4)
Residential building volume m ³ (%)	38.7 × 10 ⁶ (32.6)	47.9 × 10 ⁶ (40.4)	31.0 × 10 ⁶ (26.1)	1.0 × 10 ⁶ (0.8)
Resident population Ab (%)	61,870.2 (17.4)	169,996.4 (47.7)	119,535.8 (33.6)	4823.6 (1.4)
Summer mean LST °C (95% C.I.)	37.1 (37.1–37.1)	35.3 (35.3–35.3)	35.1 (35.1–35.1)	35.4 (35.3–35.4)
Summer mean ALB Adim. (95% C.I.)	0.240 (0.240–0.241)	0.227 (0.226–0.227)	0.228 (0.228–0.229)	0.249 (0.247–0.250)
Mean SVF Adim. (95% C.I.)	0.576 (0.576–0.577)	0.583 (0.583–0.584)	0.639 (0.638–0.640)	0.746 (0.743–0.750)

Note: 95% C.I.: confidence interval. Ab: number of inhabitants. LST: land surface temperature. ALB: albedo. SVF: sky view factor. LST and ALB values are related to residential building roofs, whereas SVF is related to 50 m buffer area surrounding residential buildings.

The highest number of residential buildings (about 43% or residential buildings of the Florentine municipality) and building dimension values were found in the semi-central belt: residential buildings surface area and volume were about 4 million m² and 48 million m³, respectively (representing slightly more than 40% of the whole residential building surface area and volume of the studied city). The lowest values were observed in the suburban belt: residential buildings accounted for less than 2% and building surface area and volume were less than 1.5% of the whole urban area studied.

Although most of the resident population (about 170,000 residents corresponding to about 48% of the Florentine population) was concentrated in the semi-central belt, the highest resident population density was observed in the central belt (8409 ab/km²), followed by the semi-central one with 4,639 ab/km², the peripheral belt with 2245 ab/km², and with the lowest value, the suburban one (943 ab/km²).

The central belt also revealed the highest summer average LST of residential building roofs (37.1 °C), whereas lower average LST values were observed for the other OMI belts (going from 35.1 °C of the peripheral belt to 35.4 °C of the suburban one).

Low albedo values of residential building roofs were observed among all OMI belts (ranging from 0.23 to 0.25) corresponding to an overall roofs' low thermal reflective property.

The lowest average SVF values calculated on a buffer area of 50 m surrounding residential buildings (shading effect caused by the urban morphology adjacent to residential buildings) were observed in central and semi-central belts (0.58), which increased to 0.64 in the peripheral belt and reaching the highest average value in the suburban one (0.75).

3.2. Residential Buildings' Real Estate Values-Related Urban Features

Similar patterns among OMI zone classes and significant associations between all urban features calculated with the two buffer areas (50 m and 100 m) were observed (Table S1 in Supplementary Materials). Significance levels (mostly $p < 0.01$) and high R-squared values (above 0.90) were generally observed considering all surface urban features (the only exception was the WB in semi-central and peripheral belts). In this study, results related to the 50 m buffer were shown with the aim to consider urban features and surface thermal patterns most proximal to residential buildings. The analyses were performed on three OMI belts (central, semi-central, and peripheral belts), whereas the suburban one was excluded because no changes in the average real estate values among residential buildings were observed within this area. In addition, the residential buildings concentration and the population density were not very represented in the suburban belt (representing less than 1.5% of the studied area).

Figure 2 represented the LST changes observed in the central (Figure 2a), semi-central (Figure 2b), and peripheral (Figure 2c) belts, according to the four OMI zone classes. Further urban features' changes (impervious area, tree cover, grassland, and water bodies) were shown in Figures S1–S4 in Supplementary Materials.

Significant linear LST decreases ($p < 0.05$) going from residential buildings with the lowest market value (OMI_C1) to buildings with the highest one (OMI_C4) were observed in the peripheral belt (Figure 2c). Significant linear IA decreases ($p < 0.01$) and TC and GA increases ($p < 0.01$ for TC and $p < 0.05$ for GA) were also observed in the peripheral belt (Supplementary Figures S1–S3).

On the other hand, no significant linear variations of LST (Figure 2) and other urban features (Supplementary Figures S1–S4) among OMI zone classes were observed in the central (Figure 2a) and semi-central (Figure 2b) belts, although in the latter case, progressive changes going from OMI_C1 to OMI_C4 were generally observed.

The highest average LST differences between the lowest and the highest market classes were almost 4 °C in the semi-central belt and about 3 °C in the peripheral one (Supplementary Table S1). The central belt showed the lowest LST differences (less than 1 °C) and very low variations of urban infrastructures frequencies (mostly less than 1%) between extreme market value classes (OMI_C1 and OMI_C4). The highest frequencies of grey and green infrastructures (with the exception of blue ones) were recorded in the semi-central and peripheral belts, showing values of 30% and 40%, respectively.

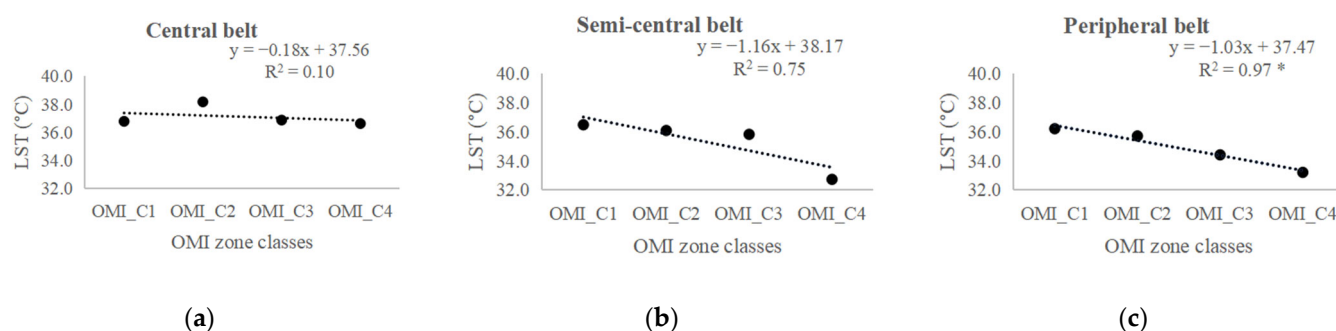


Figure 2. Land Surface Temperature (LST) distribution according to four OMI zone classes (from OMI_C1 to OMI_C4) for three different urban belts: central (a), semi-central (b) and peripheral (c). Note: Significant levels: * p -value < 0.05 .

3.2.1. Relationships between Residential Buildings' Real Estate Values and Surface Thermal Anomaly Patterns

The map referring to OMI spatial classification, residential buildings' configuration, and the surface thermal anomaly patterns of Florence is shown in Figure 3.

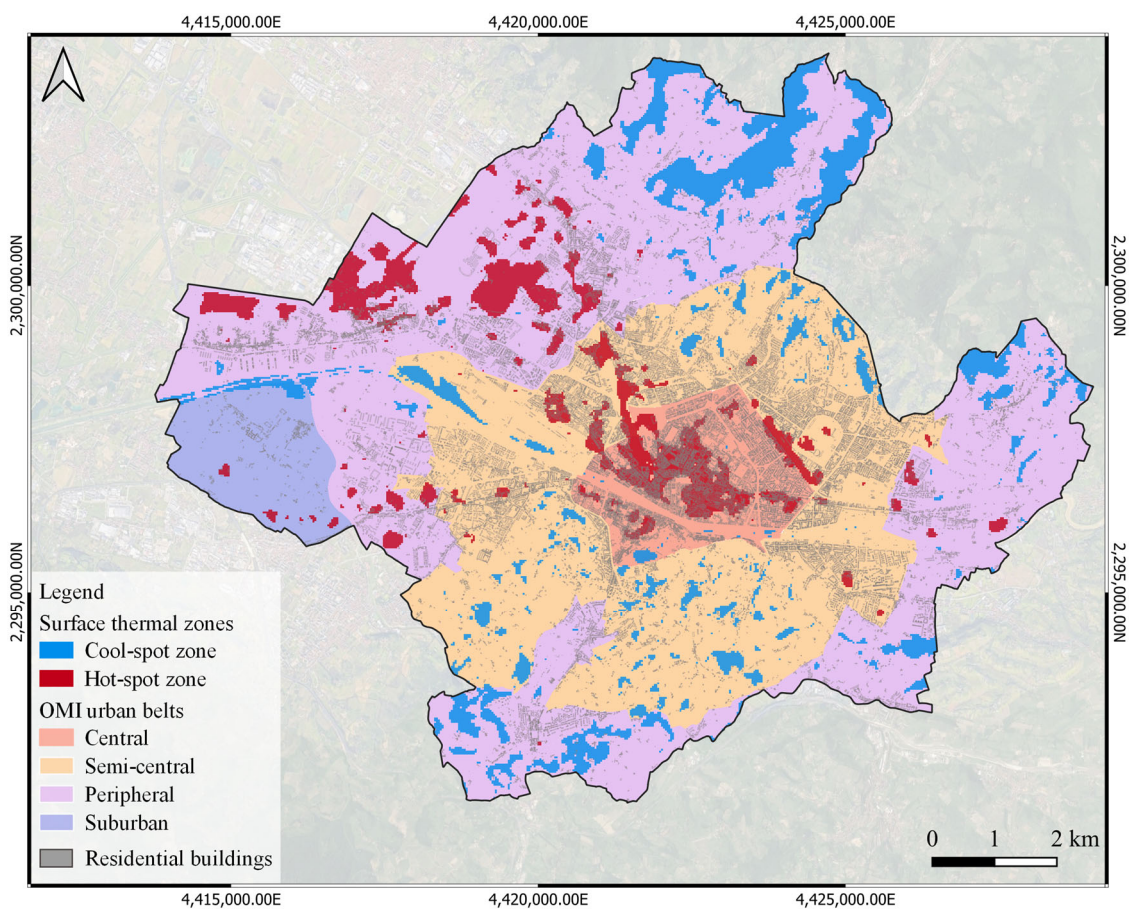


Figure 3. Surface thermal anomalies and OMI (Real Estate Market Observatory) spatial classification of residential real estate value.

The descriptive and statistical analyses regarding the relationships between residential buildings’ real estate values and surface thermal anomaly patterns are shown in Table 2.

Table 2. Descriptive and statistical analyses on the relationships between residential buildings’ real estate values and surface thermal patterns.

OMI Belt	OMI Zone Classes (OMI_C)	Residential Buildings’ Real Estate Values (euro/m ²)	Residential Buildings’ Number (%)	Residential Buildings in Hot-Spot Zones		Residential Buildings in Cool-Spot Zones	
				(%)	OR	(%)	OR
Central	OMI_C1	3175	8.0	1.2 [4.5]	0.20 (0.19–0.22) *	0 [0]	-
	OMI_C2	3175–3425	4.7	4.1 [15.5]	19.40 (17.47–21.55) *	0 [0]	-
	OMI_C3	3425–3550	9.0	2.3 [8.6]	0.46 (0.43–0.49) *	0 [0]	-
	OMI_C4	3550–4100	4.8	2.2 [8.2]	1.53 (1.42–1.64) *	<0.1 [<lt;0.1]< td=""> <td>-</td> </lt;0.1]<>	-
Semi-central	OMI_C1	2375–2700	10.5	1.4 [3.2]	9.35 (8.28–10.56) *	<0.1 [<lt;0.1]< td=""> <td>0.04 (0.01–0.15) *</td> </lt;0.1]<>	0.04 (0.01–0.15) *
	OMI_C2	2700–2750	8.0	0.2 [0.4]	0.45 (0.37–0.54) *	0 [0]	-
	OMI_C3	2750–3400	12.5	0.3 [0.8]	0.50 (0.43–0.57) *	<0.1 [<lt;0.1]< td=""> <td>0.20 (0.11–0.35) *</td> </lt;0.1]<>	0.20 (0.11–0.35) *

	OMI_C4	3400–3650	11.7	0 [0]	-	0.2 [0.7]	27.96 (16.15– 48.40) *
Peripheral	OMI_C1	1975–2300	7.6	0.6 [2.2]	2.71 (2.38–3.08) *	0 [0]	-
	OMI_C2	2300–2450	7.1	0.4 [1.4]	1.36 (1.18–1.56) *	<0.1 [<0.1]	0.08 (0.03–0.17) *
	OMI_C3	2450–2750	7.6	0.3 [1.0]	0.77 (0.66–0.89) *	0.1 [0.5]	2.41 (1.86–3.11) *
	OMI_C4	2750–3400	6.6	<0.1 [<0.1]	0.01 (0.00–0.03) *	0.2 [0.6]	3.66 (2.84–4.73) *
	Total		100	13.0		0.6	

Note: OR is the odds ratio value of each residential building falling within hot- and cool-spot zones. Percentage values are related to the total value recorded in the Florence municipal area, whereas values included in the square brackets are related to the total value recorded in each OMI belt. * $p < 0.01$.

Considering the whole Florentine municipality, 13.0% of residential buildings fell into hot-spot zones, of which 9.8% are located in the central belt (representing almost 37% of all residential buildings in the central belt) and 1.9% and 1.3% in the semi-central and peripheral belts, respectively (representing almost 4% and about 4.5% of all residential buildings in the semi-central and peripheral belts, respectively). Only 0.6% of residential buildings fell into cool-spot zones (of which about two thirds are in the peripheral belt, one third is in the semi-central one, and sporadic cases are in the central belt).

Residential buildings in the central belt with a market value belonging to OMI_C2 showed the highest frequency of falling into hot-spot zones, representing 4.1% of residential buildings in the whole Florentine municipal area and just over 15% of that of the central belt (Table 2). In this case, the odds ratio that a residential building in a hot-spot zone was significantly ($p < 0.01$) associated with a real estate value corresponding to the OMI_C2 was 19.40 times greater than buildings belonging to other market value classes. Residential buildings with the highest market value (OMI_C4) also showed a significant ($p < 0.01$) positive association ($OR > 1$) with hot-spot zones; the odds that a residential building with the highest market value fell into hot-spot zones increased by just over 50% compared to buildings with other real market values. Furthermore, buildings with the lowest real estate value (OMI_C1) revealed the lowest frequency (1.2%) of falling in hot-spot zones and a significant ($p < 0.01$) negative association with hot-spot zones; the odds that a building in a hot-spot zone was associated with the lowest market value (OMI_C1) decreased by almost 80% compared to buildings with higher real market values.

The frequency of residential buildings in the central OMI belt that fall into cool-spot zones was very low and, in any case, limited only to buildings with the highest market value (OMI_C4).

Residential buildings in semi-central and peripheral OMI belts generally revealed lower frequencies of falling into hot-spot zones than buildings in the central belt (Table 2). The highest frequencies of buildings falling into hot-spot zones always concerned those characterized by the lowest market value (OMI_C1), revealing significant ($p < 0.01$) positive associations; the odds that residential buildings with the lowest market values fell into hot-spot zones were 9.35 and 2.71 times greater than buildings belonging to higher market value classes, in semi-central and peripheral OMI belts, respectively. Negative associations ($OR < 1$) between residential buildings with the highest real estate values and hot-spot zones were observed.

Concerning buildings falling into cool-spot zones, those characterized by the highest real estate values (OMI_C4) revealed the highest frequencies and significant ($p < 0.01$) positive associations: the odds that residential buildings in cool-spot zones were associated with the highest real estate values were 27.96 and 3.66 times greater than buildings with lower market values in semi-central and peripheral OMI belts, respectively (Table 2).

3.2.2. Relationships between Real Estate Values and Urban Features Surrounding Residential Buildings

Data on urban features surrounding residential buildings (considering a buffer area of 50 m) according to three surface thermal zone (neutral, hot-spot, and cool-spot) and for each OMI belt were shown in Tables 3–5.

Table 3. The characterization of the buffer area surrounding residential buildings for three surface thermal zones (neutral, hot-spot, and cool-spot) in the OMI central belt.

Central Belt						
Surface Thermal Zones	OMI Zone Classes (OMI_C)	Frequencies of Urban Features				
		Mean ± Standard Deviation				
		LST (°C)	IA (%)	TC (%)	GA (%)	WB (%)
Neutral	OMI_C1	36.6 ^a ± 0.7	93.6 ^a ± 7.4	2.4 ^a ± 3.9	3.9 ^a ± 4.6	0.1 ^a ± 0.6
	OMI_C2	37.1 ^b ± 0.6	93.7 ^b ± 8.5	3.0 ^b ± 4.0	3.3 ^b ± 5.1	<0.1 ^a ± 0.5
	OMI_C3	36.5 ^c ± 1.1	90.7 ^c ± 11.5	4.4 ^b ± 7.2	4.5 ^a ± 5.7	0.4 ^b ± 2.6
	OMI_C4	35.4 ^d ± 1.6	85.6 ^d ± 17.8	6.3 ^b ± 10.4	5.8 ^a ± 8.7	2.4 ^c ± 6.7
	<i>p</i> -value	<0.001	<0.001	<0.001	<0.001	<0.001
Hot-spot	OMI_C1	38.0 ^a ± 0.3	99.2 ^a ± 1.7	0.3 ^a ± 0.7	0.5 ^a ± 1.5	-
	OMI_C2	38.3 ^b ± 0.3	99.4 ^b ± 1.8	0.2 ^b ± 0.9	0.4 ^b ± 1.2	-
	OMI_C3	37.9 ^c ± 0.2	99.1 ^a ± 1.9	0.4 ^a ± 1.3	0.5 ^c ± 1.1	-
	OMI_C4	38.2 ^d ± 0.3	99.9 ^c ± 0.7	<0.1 ^c ± 0.2	0.1 ^d ± 0.5	-
	<i>p</i> -value	<0.001	<0.001	<0.001	<0.001	-
Cool-spot	OMI_C1	-	-	-	-	-
	OMI_C2	-	-	-	-	-
	OMI_C3	-	-	-	-	-
	OMI_C4	30.1 ± 0.8	34.2 ± 22.7	47.0 ± 29.4	13.8 ± 9.3	5.0 ± 4.3
	<i>p</i> -value	-	-	-	-	-

Note: LST: land surface temperature. IA: impervious area. TC: tree cover. GA: grassland area. WB: water bodies. Different letters indicate statistically significant differences between OMI zone classes (*p*-value < 0.05) according to the non-parametric Mann–Whitney test.

Table 4. The characterization of the buffer area surrounding (considering a buffer of 50 m) residential buildings for three surface thermal zones (neutral, hot-spot, and cool-spot) in the OMI semi-central belt.

Semi-Central Belt						
Surface Thermal Zones	OMI Zone Classes (OMI_C)	Frequencies of Urban Features				
		Mean ± Standard Deviation				
		LST (°C)	IA (%)	TC (%)	GA (%)	WB (%)
Neutral	OMI_C1	36.3 ^a ± 1.2	88.9 ^a ± 14.0	4.0 ^a ± 7.2	7.0 ^a ± 8.6	0.1 ^a ± 1.1
	OMI_C2	36.1 ^b ± 1.0	89.3 ^a ± 13.0	3.5 ^a ± 5.8	7.0 ^b ± 9.1	0.2 ^b ± 1.9
	OMI_C3	35.8 ^c ± 1.2	87.8 ^b ± 14.6	4.6 ^b ± 7.6	7.4 ^c ± 9.2	0.1 ^c ± 0.8
	OMI_C4	32.8 ^d ± 1.6	49.3 ^c ± 23.8	27.9 ^c ± 18.4	22.7 ^d ± 14.3	<0.1 ^d ± 0.3
	<i>p</i> -value	<0.001	<0.001	<0.001	<0.001	<0.001
Hot-spot	OMI_C1	38.0 ^a ± 0.3	98.6 ^a ± 2.6	0.2 ^a ± 0.8	1.2 ^a ± 2.2	-
	OMI_C2	37.8 ^b ± 0.2	98.8 ^b ± 2.9	0.3 ^a ± 1.0	0.9 ^b ± 2.2	-
	OMI_C3	38.0 ^a ± 0.4	98.9 ^b ± 3.5	0.2 ^a ± 1.0	0.9 ^b ± 3.0	-
	OMI_C4	-	-	-	-	-
	<i>p</i> -value	<0.001	<0.001	0.370	<0.001	-
Cool-spot	OMI_C1	29.7 ^a ± 0.8	25.3 ^a ± 1.2	57.6 ^a ± 2.2	17.0 ^{ab} ± 1.0	-
	OMI_C2	-	-	-	-	-
	OMI_C3	29.6 ^a ± 0.5	45.7 ^b ± 5.7	33.7 ^b ± 8.0	20.7 ^a ± 7.8	-

OMI_C4	29.6 ^a ± 0.6	24.1 ^a ± 10.4	61.1 ^a ± 12.7	14.7 ^b ± 7.9	0.1 ± 0.7
<i>p</i> -value	0.974	<0.001	<0.001	0.046	-

Note: LST: land surface temperature. IA: impervious area. TC: tree cover. GA: grassland area. WB: water bodies. Different letters indicate statistically significant differences between OMI zone classes (*p*-value < 0.05) according to the non-parametric Mann–Whitney test.

Table 5. The characterization of the buffer area surrounding residential buildings for three surface thermal zones (neutral, hot-spot, and cool-spot) in the OMI peripheral belt.

		Peripheral Belt				
Surface Thermal Zones	OMI zone Classes (OMI_C)	Frequencies of Urban Features				
		Mean ± Standard Deviation				
		LST (°C)	IA (%)	TC (%)	GA (%)	WB (%)
Neutral	OMI_C1	36.1 ^a ± 1.0	82.0 ^a ± 15.7	4.8 ^a ± 7.4	13.2 ^a ± 11.9	0.0 ^c ± 0.5
	OMI_C2	35.6 ^b ± 1.5	72.9 ^b ± 21.9	8.3 ^b ± 11.5	18.6 ^b ± 15.0	0.2 ^a ± 1.9
	OMI_C3	34.4 ^c ± 2.1	62.4 ^c ± 28.4	14.9 ^c ± 16.8	22.6 ^c ± 18.2	0.2 ^b ± 1.2
	OMI_C4	33.3 ^d ± 1.8	55.4 ^d ± 25.8	20.4 ^d ± 16.2	24.0 ^d ± 17.2	0.2 ^{a,b} ± 1.2
	<i>p</i> -value	<0.001	<0.001	<0.001	<0.001	<0.001
Hot-spot	OMI_C1	37.8 ^a ± 0.2	96.5 ^a ± 5.1	0.5 ^a ± 1.3	3.0 ^a ± 4.6	-
	OMI_C2	38.1 ^b ± 0.6	94.6 ^b ± 7.8	0.6 ^b ± 2.0	4.8 ^b ± 6.6	-
	OMI_C3	38.0 ^b ± 0.4	95.8 ^{a,b} ± 6.5	0.3 ^{a,b} ± 0.9	3.9 ^{a,b} ± 6.2	-
	OMI_C4	37.3 ^c ± 0.0	86.6 ^b ± 8.7	4.8 ^c ± 3.9	6.4 ^{a,b} ± 3.0	2.2 ± 1.8
	<i>p</i> -value	<0.001	0.043	<0.001	0.015	-
Cool-spot	OMI_C1	-	-	-	-	-
	OMI_C2	29.5 ^a ± 1.5	26.9 ^a ± 12.3	56.0 ^a ± 18.4	16.9 ^a ± 16.1	0.3 ^a ± 0.8
	OMI_C3	29.2 ^a ± 0.8	21.1 ^a ± 9.4	59.5 ^a ± 13.1	19.1 ^a ± 11.3	0.3 ^a ± 1.2
	OMI_C4	29.1 ^a ± 0.7	23.7 ^a ± 9.2	57.4 ^a ± 13.0	18.4 ^a ± 8.4	0.5 ^a ± 2.3
	<i>p</i> -value	0.261	0.200	0.373	0.723	0.855

Note: LST: land surface temperature. IA: impervious area. TC: tree cover. GA: grassland area. WB: water bodies. Different letters indicate statistically significant differences between OMI zone classes (*p*-value < 0.05) according to the non-parametric Mann–Whitney test.

The surrounding areas of residential buildings with the highest real estate market values (OMI_C4) falling within the thermally neutral zones of central (Table 3), semi-central (Table 4), and peripheral (Table 5) belts revealed the lowest average summer LST values and IA frequencies and the highest green infrastructure surface frequencies (and of blue infrastructure, represented by water bodies, in the central belt).

On the other hand, the highest LST values were observed surrounding residential buildings associated with the real estate value corresponding to the OMI_C2 of the central belt (Table 3) and surrounding buildings characterized by the lowest real estate values (OMI_C1) of the semi-central (Table 4) and peripheral (Table 5) belts. These latter situations were also associated with high values of IA (higher or close to 90% in central and semi-central belts and 80% in the peripheral belt) and low frequencies of green infrastructures (just over 5% in central belt, close to 10% in the semi-central belt, and less than 20% in the peripheral belt).

The highest significant (*p* < 0.05) summer average LST difference among residential buildings falling in the thermal neutral zone of the central belt (Table 3) was observed between buildings classified as OMI_C2 and OMI_C4 (1.7 °C). All urban infrastructures revealing maximum differences among OMI zone classes were always lower than 10%, showing the lowest difference for WB. In particular, TC, GA, and WB were always found to be higher in the surrounding areas of residential buildings with the highest real estate market values (OMI_C4).

A much less marked variability among OMI zone classes was instead observed concerning urban features surrounding residential buildings that fell into hot-spot zones. In

particular, variations of LST always lower than 0.5 °C (the LST in hot-spot zones increased by about 1.8 °C compared to thermally neutral zones, settling on values of about 38 °C in all OMI zone classes, Table 3) and 1% for the various urban infrastructures were observed. The IA surrounding residential buildings in hot-spot zones increased on average of about 8.4% (settling on values higher than 99% in all OMI zone classes, Table 3), whereas TC and GA decreased by 3.6% and 4.1%, respectively (settling on values always lower than 0.5% in all OMI zone classes, Table 3), compared to residential buildings in thermally neutral zones. No water bodies were observed surroundings residential buildings falling in hot-spot zones of the central belt (Table 3).

The urban features surrounding residential buildings located in the thermally neutral zone especially in the semi-central (Table 4), but also in the peripheral (Table 5) belts, revealed greater variability among the various OMI zone classes than buildings in the central (Table 3) belt. The highest significant ($p < 0.05$) LST differences were observed between buildings characterized by the lowest and highest real estate market values (OMI_C1 and OMI_C4 respectively): 3.5 °C and 2.8 °C in semi-central and peripheral belts, respectively. High significant variations of all urban infrastructure frequencies among OMI zones were also observed in both semi-central and peripheral belts: maximum differences between OMI zones were always higher than 10%, 15%, and 25% for GA, TC, and IA, respectively, whereas very little maximum differences were observed for WB (lower than 0.5%).

These variations were often linear and statistically significant in the peripheral belt going from buildings characterized by the lowest real estate value class (OMI_C1) to the highest one (OMI_C4); significant linear decreases of LST ($R^2 = 0.9743$; $p < 0.05$) and IA ($R^2 = 0.9941$; $p < 0.01$) and increases of TC ($R^2 = 0.9862$; $p < 0.01$) and GA ($R^2 = 0.9399$; $p < 0.05$) were observed.

Even in this case, as for the central belt, much less marked variability of average LST values among OMI zone classes was observed in hot-spot zones, with maximum LST variations of 0.2 °C and 0.8 °C in semi-central and peripheral belts, respectively. Little maximum variations between OMI zone classes were also observed for the various urban infrastructures; variations always lower than 1% and 10% were observed when semi-central and peripheral belts were considered.

The frequency variations of urban infrastructures surrounding residential buildings in hot-spot zones compared to residential buildings in thermally neutral zones changed more in semi-central and especially in peripheral belts than in the central belt. In particular, the IA surrounding residential buildings in hot-spot zones of the peripheral belt increased on average of about 27% (settling on values higher than 85% in all OMI zone classes, Table 5), whereas TC and GA decreased by about 11% and 16%, respectively (settling on values always lower than 7% in all OMI zone classes, Table 5), compared to residential buildings in thermally neutral zones.

As for the central belt, no water bodies were observed surrounding residential buildings falling in hot-spot zones of the semi-central belt (Table 4), whereas a low frequency (2.2%) was only observed in surrounding buildings with the highest real estate market value (OMI_C4) of the peripheral belt (Table 5).

The very few residential buildings that fell into cool-spot zones belonged especially to the OMI zone class characterized by the highest real estate market value (OMI_C4) (Tables 3–5). Residential buildings in cool-spot zones revealed a decrease of the surrounding LST of just over 5 °C and of IA frequencies of above 40% compared to buildings in the thermally neutral zones, counterbalanced by increases of frequencies of surrounding green infrastructures (the sum of TC and GA) and, to a lesser extent, of WB.

4. Discussion

The originality of this work is that of having investigated a phenomenon that is still little or not at all explored: the relationships between residential buildings' real estate values in an historical Italian city, intra-urban surface thermal anomaly patterns (in particular

the spatial distribution of hot- and cool-spot zones), urban features useful for the evaluation of the physical characteristics of residential buildings, and the infrastructure composition of buildings' surroundings. The research proposed in this study has the strength of being based on the use of open spatial data managed by national (the Real Estate Market Observatory of the Italian National Revenue Agency, the Italian National Institute of Statistics and the National Institute for Environmental Protection and Research) and international (remote sensing products from NASA and Copernicus missions) reference organizations. For this reason, the study is easily replicable and extendable to other urban areas.

Interesting studies dealing with the relationships between real estate values and different environmental elements, including the distance from green areas, proximity to center and water bodies, by using remote sensing and GIS data, are already available in the scientific literature [19,43–46]. However, few studies have investigated the intra-urban surface thermal anomaly pattern in relation to the real estate value of residential buildings, and in particular those aimed at investigating the relationship between surface thermal hot-spot zones, a phenomenon that increasingly affects our cities, and the real estate market value.

This aspect is of particular importance since temperatures are increasing globally due to the climate change phenomenon [2], with significant impacts on many aspects of human life and often devastating damages to ecosystems [47]. The effects are known to be particularly critical in urban areas due to the complex mix of urban infrastructures, which tend to modify the urban energy balance, trapping the heat and favoring the creation of an articulated intra-urban thermal mosaic characterized by areas that can present important surface thermal anomalies and threaten not only human health [48,49] but also urban infrastructures [50,51], and causing important economic repercussions. These latter issues could be potentially linked to energy and water consumption [52,53], in addition to an increase in conditions of thermal discomfort affecting the quality of life even outside the typically hot period. A seasonal adjustment of abnormal warm conditions was also observed in many European areas affecting other periods of the year and seasons outside the typically hot summer one [54]. A study conducted on European cities [55] demonstrated an increasing LST trend in the last decade, and also showed that the recent three-year (2018–2020) average urban LST maxima (35.8 °C) of 1.4 °C is higher than 20 years ago.

Considering the increase in frequency, high intensity, and long duration of heat waves, also highlighted in many European cities located especially in the central and southern European areas [12], we are aware that the real estate market will also certainly be negatively affected. Actions addressed to improve the building performance resilience from a thermal perspective [56] will represent a priority strategy to avoid property devaluations with direct impacts on residential building real estate market. A previous study conducted in the city of Wuhan in China [19] found that LST is significantly and negatively correlated with housing prices, indicating that the urban thermal environment can represent urban disservices to some extent. This topic is of particular importance if we consider the cultural aspects that affect the area under study. Italy is characterized, in large part, by “homeowners” (slightly more than 70% in 2019 were owners based on the web platform “Statista” specializing in market and consumer data) interested in preventing any real estate market devaluation. This study could have strong public policy implications giving general indications and highlighting critical urban features that could worsen future thermal patterns, and potentially affect the residential building real estate value.

Considering the Florence municipality, semi-central and peripheral belts revealed progressive changes of LST and most of the analyzed urban features going from the lowest to the highest residential building real estate value often showed statistically significant linear variations in the peripheral belt. In these areas, therefore, where the urban fabric was not relevant from a historical and architectural point of view, the thermal pattern and the urban surface features (grey, green, and blue surfaces) revealed a linear association with the real estate value. On the other hand, the lack of identification of a clear relationship between urban features and residential building real estate values in the central belt was due to additional factors, above all connected with the proximity to areas of great

historical, cultural, and architectural interest, as already demonstrated by a previous study conducted at regional scale on Tuscany (Italy) [57]. Our analysis showed that the LST was a determining factor in evaluating the residential building real estate value moving away from the city center. The effects were evident in the semi-central and peripheral belts, and in the latter, the association was linearly significant; going from residential buildings with the lowest market value (OMI_C1) to buildings with the highest one (OMI_C4), an average reduction of grey surfaces of about 30% was associated with an average increase in green surfaces of almost 30% (17% of TC and 12% of GA), which determined an average reduction of the summer LST of about 3 °C. The highest LST reduction (about 4 °C) was recorded in the semi-central belt. On the other hand, the LST was not considered a determining factor clearly modifying the residential real estate value in the central belt. In this case, it is very likely that additional elements in the central belt (such as the proximity to important places from the historical, landscape, and architectural point of view) affect the real estate market value of the central core of Florence.

The thermal hot-spot analysis provided an important and original contribution to describe the relationship between the real estate value and the urban thermal pattern. This is a topic that needs increasing attention in a period in which our planet is affected by a generalized global warming and whose effects are exacerbated in urban areas.

It is clearly evident that approximately 37% of all residential buildings in the central belt (that are also those with the highest real estate market values in Florence) and which fall into surface hot-spot zones (a focus on the latter is shown in Figure 4) are surrounded almost exclusively by impervious surfaces (representing more than 99% of urban infrastructures in all OMI zone classes).

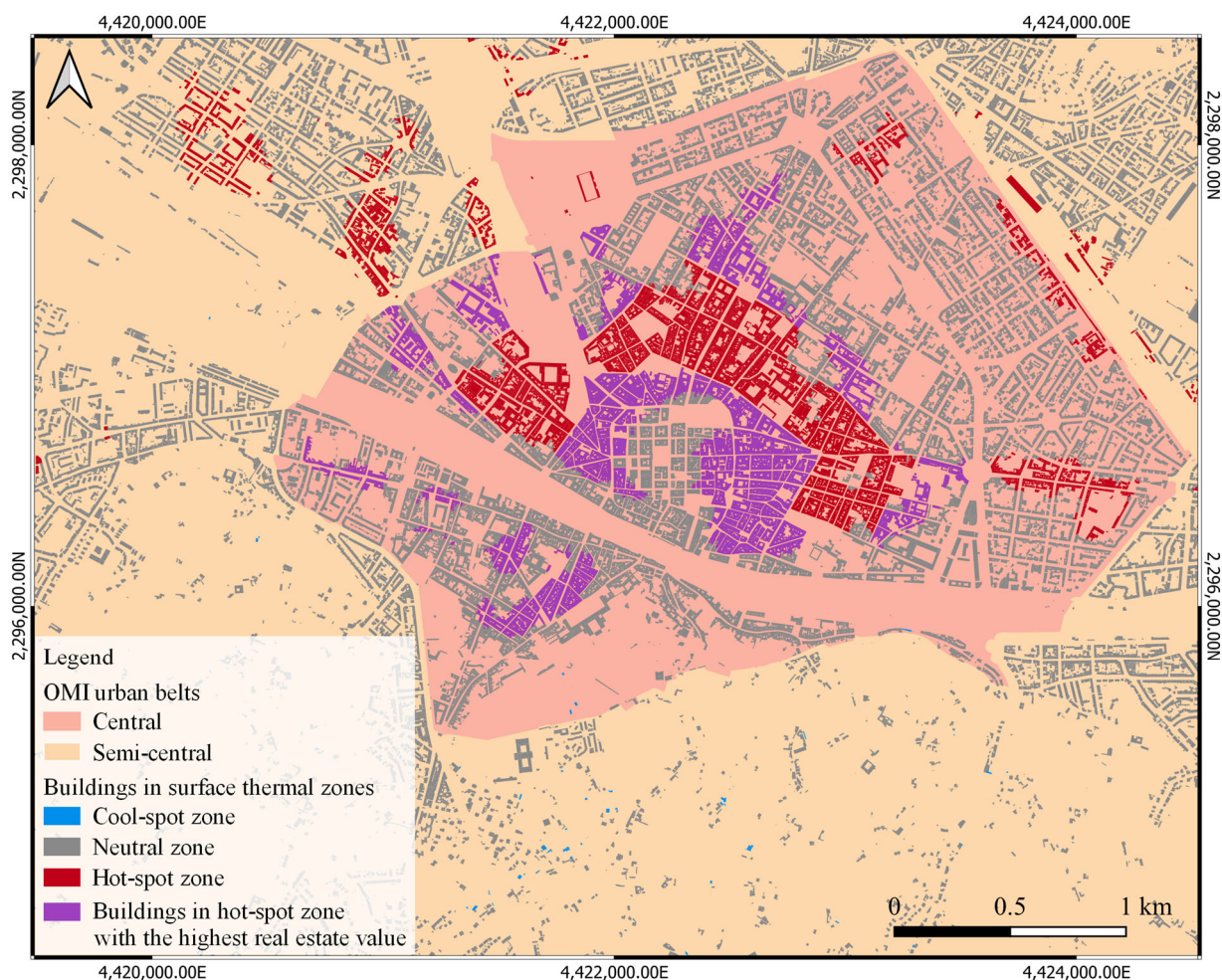


Figure 4. Focus on the residential buildings falling into hot-spot zones of the central belt.

Contrary to the hypothesis of our study, residential buildings with the highest market value (OMI_C4) in the central belt (indicated in purple color in Figure 4 and representing just over 20% of all central belt buildings) revealed a significant positive association with hot-spot zones. The average LST surrounding these buildings was significantly higher than that of surrounding buildings that fell into other surface thermal zones (2 °C or even 8 °C higher than buildings in thermally neutral or cool zones respectively), despite having the same real estate market values. This is justified by findings from a recent study [57] exploring the relationships between the real estate value in Tuscany (Italy) and the proximity to services (the distance from urban center and roads), which revealed a high correlation in the municipal area of Florence.

Results from our study revealed that even slight increases of green and blue infrastructure in the proximity of residential buildings can significantly improve the thermal situation, reducing the summer average LST almost by about 2 °C (e.g., obtained simply by increasing the surface surrounding the building with about 4% of TC and GA) or even more in the case of greater presence of green infrastructures.

These findings are also supported by previous studies demonstrating that the proximity of green and blue infrastructures have an impact on apartment prices [43,46,58–61]. A recent study conducted on the city of Lisbon [60] demonstrated that for a square kilometer increase in relative tree canopy coverage of a neighborhood, the impact would cost on average approximately EUR 400 per dwelling.

Results from the present study clearly highlight that residential buildings falling into hot-spot zones represent the priority to plan interventions because they are exposed to greater economic impacts. In particular, potential repercussions on the real estate market in the near future are trusted. Heat-related direct influences on the thermal performance of buildings are expected because of the decrease in efficiency of energy systems, with consequent significant increases in the risk of building energy consumption and power outages, water demand, and worsening of indoor thermal comfort [50,62]. Above all, for buildings in hot-spot zones, the need for resilient building design is urgent and it represents one of the main challenges in the building industry. The planning of well-integrated interventions that respect the historical, cultural, and architectural contexts of the city of Florence are therefore strongly needed.

Interventions aimed at increasing the building thermal insulation, cool/green roofs and facades, solar shading/glazing, ventilated roofs and facades, cool envelope materials, and the organization of the space in the proximity of buildings by using nature-based solutions (such as the presence of trees that increases air flow and reduces the impact of solar radiation) represent some example of strategies to mitigate buildings coping with excessive heat in hot-spot zones and buildings overheating, which represent a threat to the health and life of occupants [62,63]. A combination of cooling strategies with different capacities is important to obtain resilient cooling (by using low-energy and low-carbon cooling solutions) of buildings [63]. These building-related resilient strategies represent the main aim of actions against climate change and the consequent hazards addressed by the recently formed International Energy Agency (IEA) Energy in Buildings and Community Programme (EBC) Annex 80 “Resilient Cooling of Buildings” [64]. The recent report of the United Nations Environment Programme [65] on recognizing the key role buildings can play in enhancing climate change adaptation, improving resilience, and addressing and mitigating risk, also demonstrated how combining grey building solutions with green nature-based solutions can have promising results.

The statistically significant heterogeneity of LST values and of various urban infrastructures generally observed in this study among buildings belonging to different real estate market value classes (with the exception of buildings that fell into cool-spot areas especially in the peripheral area) demonstrates the importance of these elements in addition to those already considered by the Italian OMI for classifying areas with homogeneous residential building real estate values: the average year of construction, the number

of floors, the surface area, the presence of public and commercial services, public green, parking, the level of the transport services, road connections, and commercial vocation.

The implementation of the elements considered in this study in the OMI classification procedures of real estate market values, and of the information relating to the intra-urban surface thermal anomaly pattern, are certainly facilitated by the fact that these results were obtained from processing open source data and therefore are easily extendable and replicable to the whole national territory.

As future climate projections show that our urban environments will be increasingly exposed to intense and prolonged periods of intense heat, it is crucial to consider the intra-urban thermal pattern when evaluating real estate. Increased attention must be addressed to targeted building intervention strategies to avoid significant local economic repercussions due to a probable decrease in the value of residential properties in areas characterized by high heat-related risk.

Study Limitation

This study showed some limitations related to the resolution of remote sensing data (Landsat-8) used for the LST calculation (resampled from 100 m to 30 m horizontal resolution by the USGS). It was recognized that the cubic convolution resampling by the USGS on TIRS data can be considered a limitation since it may lead to uncertainty in remote sensing-based LST measurement when conducting pixel-scale validation [30], especially for analysis at the building level. Despite the Landsat-8 remote sensing data showing one of the best resolutions available using open data sources, better performance may be achieved when higher resolution data will be available.

Furthermore, our study investigated the daytime surface thermal pattern with the aim to study the surface thermal extremes typically occurring during daytime and in the summer period; however, focusing on other periods, such as nighttime and also the winter period, can be of great interest for urban studies.

A further limitation is represented by the different recording periods used for urban characteristics and real estate value data, in any case, all attributable to the last 5 years. However, it should be highlighted that no major changes have taken place in the urban fabric of Florence in the last 5 years, and therefore no substantial variation of the real estate value was recorded. In addition, our work only focused on urban surfaces' characteristics and did not investigate further potential factors affecting real estate values, such as the temporal changes of buildings and landscape. Therefore, our future studies will also focus on these dynamics, especially on the urban and green gentrification, already explored in recent studies by using remote sensing data [66,67].

We are aware of the limitation of our study due to the buffer area size which restricts the analysis within 50 m of distance and introduces an arbitrary element as a function of the building size. However, previous studies applied similar buffer areas to evaluate the influence of the daytime summer LST on urban feature concentrations surrounding residential and industrial buildings [21,42]. As reported by recent studies [21,37,40,68,69], favorable buffers ranging from about 50 m and 300 m were used to investigate the potential LST-related thermal drivers on local urban scales.

Moreover, we are aware that different approaches for surface types' classification (also based on different NDVI thresholds) are available [70]. Therefore, in our study the surface layers developed by the National reference body (ISPRA) proposed for these purposes were used.

In addition, this study did not investigate further urban elements (such as buildings' physical structure and material, the proximity to services, road infrastructure, and historic buildings) which potentially affect real estate values. However, much of this information has already been considered in the OMI real estate value classification, whereas others, when freely available, could be considered in future studies.

5. Conclusions

This study made it possible to investigate a phenomenon that is still very little explored, and which represents an emerging problem that will be increasingly impacted from an economic point of view in the near future. The study of the relationships between the real estate value of residential buildings and the complex intra-urban surface thermal hot-spot pattern, accounting for the influence of urban features, is a priority in light of climate change projections.

The research hypothesis of this study, that the increase in the real estate value of residential buildings is associated with the improvement of the surface thermal pattern and a greater concentration of green-blue infrastructures in the proximity of residential buildings, was not confirmed throughout the whole municipal area (instead confirmed in the peripheral belt).

Our analysis showed that the LST was a determining factor in evaluating the residential building real estate value moving away from the city center. The effects were evident in the semi-central and peripheral belts, and the association was linearly significant, especially in the latter. The LST showed no significant linear correlation with the residential real estate value in the central belt and this explained that the Italian real estate market did not consider the LST as a factor in evaluating the prices [29]. Therefore, it was very likely that additional elements (such as the proximity to important places from the historical, landscape and architectural point of view) affected the real estate market of the central core of Florence. However, the thermal hot-spot analysis revealed the highest density of residential building falling into hot-spot zones in the central core. In addition, under the urban climate scenarios exacerbated by the climate change effects, there will be an increasing need for the real estate market in evaluating the housing prices by considering specific characteristics of urban surfaces (such as the surface thermal hot-spot patterns) affecting the microclimate of the urban environment.

However, the study revealed that about 37% of residential buildings in the central belt fell into thermally hot-spot zones. Of these buildings, almost 10% (representing just over 20% of all central belt buildings) belonged to the class with the highest market value (OMI_C4), revealing a positive association (OR = 1.53) with hot-spot zones compared to buildings with other real estate values in the same area. The average LST value surrounding buildings in hot-spot zones was significantly higher (from 2 °C to 8 °C), and almost entirely affected by impervious surfaces than buildings falling into other surface thermal zones, despite belonging to the same real estate market value. This means that the LST surrounding residential buildings in hot-spot zones was the highest regardless of the market value. However, it has been observed that when buildings have even slightly higher concentrations of green or blue infrastructures in the surrounding areas, the situation significantly improves. Our results underline that, considering the future scenarios exacerbated by climate change, it is crucial to consider detailed intra-urban thermal patterns when evaluating the real estate market.

The accurate identification of residential buildings, accounting for their real estate value, that fall into hot-spot zones and the knowledge of the urban features surrounding these buildings, allows for obtaining precious information for policy makers, public authorities, and urban planners. This information is useful to plan targeted building interventions, and to the spaces in the proximity of the building with the aim to make buildings sustainable and more energy efficient, and avoids future depreciation of residential building real estate value due to the heat effects (increasing operational costs at real estate assets linked to energy and water consumption and increasing of thermal discomfort) and because consumer preferences shift. The consequent economic damage could be particularly significant since an overwhelming majority of Italians (slightly more than 70% in 2019) live in an owner-occupied home and residential is the largest sector in the Italian real estate market.

The possibility of using open data to identify the intra-urban surface thermal hot-spot areas and to characterize and quantify the infrastructures in the proximity of buildings will allow for the replicability of the analyses to other cities in different geographical contexts as well as being easily implemented in the procedures for the attribution of the most appropriate real estate market value.

The main questions for addressing future studies are the following:

- What will happen to the real estate value of residential buildings falling into hot-spot zones if targeted actions are not planned?
- Will the attractiveness and charm of a residential building located in a historical, cultural, and architectural context be able to continue to prevail over the increasingly higher operational costs at real estate assets necessary to ensure a good quality of life in specific areas of the city characterized by significant temperature increases?

Therefore, organizations responsible for the economic evaluation of the real estate value of residential buildings should also take more responsibility for intra-urban thermal anomalies and, in particular, the presence of hot-spots potentially leading to economic repercussions. Future steps will be targeted to numerical simulations of urban resilient building interventions currently falling into hot-spot zones, respecting the city-specific historical and architectural characteristics.

Supplementary Materials: The following supporting information can be downloaded at: www.mdpi.com/article/10.3390/su14148412/s1, Figure S1. Impervious area (IA) according to four OMI zone classes (from OMI_C1 to OMI_C4) for three different urban belts: central (a), semi-central (b), and peripheral (c). Figure S2. Tree cover (TC) according to four OMI zone classes (from OMI_C1 to OMI_C4) for three different urban belts: central (a), semi-central (b), and peripheral (c). Figure S3. Grassland area (GA) according to four OMI zone classes (from OMI_C1 to OMI_C4) for three different urban belts: central (a), semi-central (b), and peripheral (c). Figure S4. Water bodies (WB) according to four OMI zone classes (from OMI_C1 to OMI_C4) for three different urban belts: central (a), semi-central (b), and peripheral (c). Table S1. Comparisons between surface urban features in two buffer areas (calculated with a radius of 50 m and 100 m) surrounding residential buildings in the three different OMI belts (central, semi-central and peripheral).

Author Contributions: Conceptualization, G.G., A.C., and M.M. (Marco Morabito); methodology, G.G., A.C., I.C., L.C., and M.M. (Marco Morabito); software, G.G. and A.C.; formal analysis, G.G. and I.C.; investigation, G.G., A.C., M.M. (Michele Munafò), and M.M. (Marco Morabito); data curation, A.C., L.C., M.M. (Michele Munafò), and M.M. (Marco Morabito); writing—original draft preparation, G.G. and M.M. (Marco Morabito); writing—review and editing, A.C., I.C., L.C., and M.M. (Michele Munafò); supervision, A.C. and M.M. (Marco Morabito). All authors have read and agreed to the published version of the manuscript.

Funding: This research received no external funding.

Institutional Review Board Statement: Not applicable.

Informed Consent Statement: Not applicable.

Data Availability Statement: Data used in this study is available in a public repository on the Zenodo platform (<https://doi.org/10.5281/zenodo.5807345>).

Acknowledgments: The authors acknowledge the USGS-NASA and the European Space Agency for providing Landsat 8 data and Sentinel-2A products related to the summer period from 2015 to 2019. Special thanks to the Italian National Institute for Environmental Protection and Research (ISPRA) for providing the high-resolution tree cover, grassland, and impervious surface layers used in this study. The authors also thank the National Revenue Agency of Italy and the Tuscany Region database (GEOscopio Platform) for providing residential buildings' real estate values and feature layers.

Conflicts of Interest: The authors declare no conflict of interest.

Abbreviations

LST	Land surface temperature
IA	Impervious area
TC	Tree cover
GA	Grassland area
WB	Water bodies
SVF	Sky View Factor
OMI	Real Estate Market Observatory of the National Revenue Agency of Italy
OMI_C	OMI zone classes: ranging from OMI_C1 to OMI_C4 with the lowest of the highest residential building real estate values, respectively

References

- Hjort, J.; Streletskiy, D.; Doré, G.; Wu, Q.; Bjella, K.; Luoto, M. Impacts of permafrost degradation on infrastructure. *Nat. Rev. Earth Environ.* **2022**, *3*, 24–38. <https://doi.org/10.1038/s43017-021-00247-8>.
- World Meteorological Organization. *The Global Climate in 2015–2019*; World Meteorological Organization (WMO): Geneva, Switzerland, 2020. Available online: https://library.wmo.int/doc_num.php?explnum_id=10251 (accessed on 6 June 2022).
- Mirzaei, M.; Verrelst, J.; Arbabi, M.; Shaklabadi, Z.; Lotfizadeh, M. Urban Heat Island Monitoring and Impacts on Citizen's General Health Status in Isfahan Metropolis: A Remote Sensing and Field Survey Approach. *Remote Sens.* **2020**, *12*, 1350. <https://doi.org/10.3390/rs12081350>.
- Battaglia, J.M.A.; Douglas, S.; Hennigan, C.J. Effect of the Urban Heat Island on Aerosol pH. *Environ. Sci. Technol.* **2017**, *51*, 13095–13103. <https://doi.org/10.1021/acs.est.7b02786>.
- Heaviside, C.; Macintyre, H.; Vardoulakis, S. The Urban Heat Island: Implications for Health in a Changing Environment. *Curr. Environ. Health Rep.* **2017**, *4*, 296–305. <https://doi.org/10.1007/s40572-017-0150-3>.
- Akbari, H.; Kolokotsa, D. Three decades of urban heat islands and mitigation technologies research. *Energy Build.* **2016**, *133*, 834–842. <https://doi.org/10.1016/j.enbuild.2016.09.067>.
- Amirtham, L.R.; Devadas, M.D.; Perumal, M.; Amirtham, L. Mapping of Micro-Urban Heat Islands and Land Cover Changes: A Case in Chennai City, India. *Int. J. Clim. Chang. Impacts Responses* **2009**, *1*, 71–84. <https://doi.org/10.18848/1835-7156/cgp/v01i02/37258>.
- Smargiassi, A.; Goldberg, M.S.; Plante, C.; Fournier, M.; Baudouin, Y.; Kosatsky, T. Variation of daily warm season mortality as a function of micro-urban heat islands. *J. Epidemiol. Community Health* **2009**, *63*, 659–664. <https://doi.org/10.1136/jech.2008.078147>.
- Stathopoulou, M.; Cartalis, C.; Keramitsoglou, I. Mapping micro-urban heat islands using NOAA/AVHRR images and CORINE Land Cover: An application to coastal cities of Greece. *Int. J. Remote Sens.* **2004**, *25*, 2301–2316. <https://doi.org/10.1080/01431160310001618725>.
- Perkins-Kirkpatrick, S.E.; Lewis, S.C. Increasing trends in regional heatwaves. *Nat. Commun.* **2020**, *11*, 1–8. <https://doi.org/10.1038/s41467-020-16970-7>.
- Smid, M.; Russo, S.; Costa, A.C.; Granell, C.; Pebesma, E. Ranking European capitals by exposure to heat waves and cold waves. *Urban Clim.* **2019**, *27*, 388–402. <https://doi.org/10.1016/j.uclim.2018.12.010>.
- Morabito, M.; Crisci, A.; Messeri, A.; Messeri, G.; Betti, G.; Orlandini, S.; Raschi, A.; Maracchi, G. Increasing Heatwave Hazards in the Southeastern European Union Capitals. *Atmosphere* **2017**, *8*, 115. <https://doi.org/10.3390/atmos8070115>.
- Tyndall, J. Sea Level Rise and Home Prices: Evidence from Long Island. *J. Real Estate Financ. Econ.* **2021**, 1–27. <https://doi.org/10.1007/s11146-021-09868-8>.
- Kim, S.K.; Peiser, R.B. The implication of the increase in storm frequency and intensity to coastal housing markets. *J. Flood Risk Manag.* **2020**, *13*, e12626. <https://doi.org/10.1111/jfr3.12626>.
- Atreya, A.; Czajkowski, J. Graduated Flood Risks and Property Prices in Galveston County. *Real Estate Econ.* **2016**, *47*, 807–844. <https://doi.org/10.1111/1540-6229.12163>.
- Rossi, A.J. *Wildfire Risk and the Residential Housing Market: A Spatial Hedonic Analysis*; College Undergraduate Research Electronic Journal, University of Pennsylvania: Philadelphia, PA, USA, 2014. Available online: <https://repository.upenn.edu/curej/178> (accessed on 7 June 2022).
- Ewing, B.T.; Kruse, J.B.; Wang, Y. Local housing price index analysis in wind-disaster-prone areas. *Nat. Hazards* **2006**, *40*, 463–483. <https://doi.org/10.1007/s11069-006-9005-1>.
- Loomis, J. Do nearby forest fires cause a reduction in residential property values? *J. For. Econ.* **2004**, *10*, 149–157. <https://doi.org/10.1016/j.jfe.2004.08.001>.
- Jiao, L.; Xu, G.; Jin, J.; Dong, T.; Liu, J.; Wu, Y.; Zhang, B. Remotely sensed urban environmental indices and their economic implications. *Habitat Int.* **2017**, *67*, 22–32. <https://doi.org/10.1016/j.habitatint.2017.06.012>.
- Guerri, G.; Crisci, A.; Messeri, A.; Congedo, L.; Munafò, M.; Morabito, M. Thermal Summer Diurnal Hot-Spot Analysis: The Role of Local Urban Features Layers. *Remote Sens.* **2021**, *13*, 538. <https://doi.org/10.3390/rs13030538>.
- Guerri, G.; Crisci, A.; Congedo, L.; Munafò, M.; Morabito, M. A functional seasonal thermal hot-spot classification: Focus on industrial sites. *Sci. Total Environ.* **2021**, *806*, 151383. <https://doi.org/10.1016/j.scitotenv.2021.151383>.

22. Rubel, F.; Kotteck, M. Observed and projected climate shifts 1901–2100 depicted by world maps of the Köppen-Geiger climate classification. *Meteorol. Z.* **2010**, *19*, 135–141. <https://doi.org/10.1127/0941-2948/2010/0430>.
23. Munafò, M. (Ed.) *Consumo di Suolo, Dinamiche Territoriali e Servizi Ecosistemici*; Report ISPRA; 2020; Volume 15; ISBN 978-88-448-1013-9. Available online: <https://www.snpambiente.it/2020/07/22/consumo-di-suolo-dinamiche-territoriali-e-servizi-ecosistemici-edizione-2020/> (accessed on 7 June 2022).
24. QGIS Development Team. QGIS Geographic Information System. Open Source Geospatial Foundation Project. 2018. Available online: <http://qgis.osgeo.org> (accessed on 11 March 2022).
25. IBM Corp. *IBM SPSS Statistic for Windows, Version 27.0*; IBM Corp: Armonk, NY, USA, 2019.
26. Voogt, J.A.; Oke, T.R. Thermal remote sensing of urban climates. *Remote Sens. Environ.* **2003**, *86*, 370–384. [https://doi.org/10.1016/s0034-4257\(03\)00079-8](https://doi.org/10.1016/s0034-4257(03)00079-8).
27. Chakraborty, T.; Lee, X. A simplified urban-extent algorithm to characterize surface urban heat islands on a global scale and examine vegetation control on their spatiotemporal variability. *Int. J. Appl. Earth Obs. Geoinf. ITC J.* **2018**, *74*, 269–280. <https://doi.org/10.1016/j.jag.2018.09.015>.
28. Miles, V.; Esau, I. Surface urban heat islands in 57 cities across different climates in northern Fennoscandia. *Urban Clim.* **2020**, *31*, 100575. <https://doi.org/10.1016/j.uclim.2019.100575>.
29. Festa, M.; Longhi, S.; Cantone, G.; Papa, F. *Manuale della Banca dati Quotazioni Dell’osservatorio del Mercato Immobiliare. Istruzioni Tecniche per la Formazione della Banca Dati Quotazioni OMI*; Agenzia delle Entrate: Rome, Italy, 2017. Available online: <https://www.agenziaentrate.gov.it/wps/content/nsilib/nsi/schede/fabbricatiterreni/omi/manuali+e+guide> (accessed on 6 June 2022).
30. Bonafoni, S.; Sekertekin, A. Albedo Retrieval from Sentinel-2 by New Narrow-to-Broadband Conversion Coefficients. *IEEE Geosci. Remote Sens. Lett.* **2020**, *17*, 1618–1622. <https://doi.org/10.1109/lgrs.2020.2967085>.
31. Daramola, M.T.; Balogun, I.A. Analysis of the urban surface thermal condition based on sky-view factor and vegetation cover. *Remote Sens. Appl. Soc. Environ.* **2019**, *15*, 100253. <https://doi.org/10.1016/j.rsase.2019.100253>.
32. Dirksen, M.; Ronda, R.; Theeuwes, N.; Pagani, G. Sky view factor calculations and its application in urban heat island studies. *Urban Clim.* **2019**, *30*, 100498. <https://doi.org/10.1016/j.uclim.2019.100498>.
33. Bernard, J.; Bocher, E.; Petit, G.; Palominos, S. Sky View Factor Calculation in Urban Context: Computational Performance and Accuracy Analysis of Two Open and Free GIS Tools. *Climate* **2018**, *6*, 60. <https://doi.org/10.3390/cli6030060>.
34. Oke, T.R. Canyon geometry and the nocturnal urban heat island: Comparison of scale model and field observations. *J. Clim.* **1981**, *1*, 237–254. <https://doi.org/10.1002/joc.3370010304>.
35. Ord, J.K.; Getis, A. Local Spatial Autocorrelation Statistics: Distributional Issues and an Application. *Geogr. Anal.* **1995**, *27*, 286–306. <https://doi.org/10.1111/j.1538-4632.1995.tb00912.x>.
36. Morabito, M.; Crisci, A.; Messeri, A.; Orlandini, S.; Raschi, A.; Maracchi, G.; Munafò, M. The impact of built-up surfaces on land surface temperatures in Italian urban areas. *Sci. Total Environ.* **2016**, *551–552*, 317–326. <https://doi.org/10.1016/j.scitotenv.2016.02.029>.
37. Morabito, M.; Crisci, A.; Georgiadis, T.; Orlandini, S.; Munafò, M.; Congedo, L.; Rota, P.; Zazzi, M. Urban Imperviousness Effects on Summer Surface Temperatures Nearby Residential Buildings in Different Urban Zones of Parma. *Remote Sens.* **2017**, *10*, 26. <https://doi.org/10.3390/rs10010026>.
38. Munafò, M. (Ed) *Consumo di Suolo, Dinamiche Territoriali e Servizi Ecosistemici*; Report ISPRA; 2018, Volume 288; ISBN 978-88-448-0902-7. Available online: <https://www.isprambiente.gov.it/it/pubblicazioni/rapporti/consumo-di-suolo-dinamiche-territoriali-e-servizi-ecosistemici-edizione-2018> (accessed on 7 June 2022).
39. Strollo, A.; Smiraglia, D.; Bruno, R.; Assennato, F.; Congedo, L.; de Fioravante, P.; Giuliani, C.; Marinosci, I.; Riitano, N.; Munafò, M. Land consumption in Italy. *J. Maps* **2020**, *16*, 113–123. <https://doi.org/10.1080/17445647.2020.1758808>.
40. Morabito, M.; Crisci, A.; Guerri, G.; Messeri, A.; Congedo, L.; Munafò, M. Surface urban heat islands in Italian metropolitan cities: Tree cover and impervious surface influences. *Sci. Total Environ.* **2020**, *751*, 142334. <https://doi.org/10.1016/j.scitotenv.2020.142334>.
41. Mann, H.B.; Whitney, D.R. On a Test of Whether one of Two Random Variables is Stochastically Larger than the Other. *Ann. Math. Stat.* **1947**, *18*, 50–60. <https://doi.org/10.1214/aoms/1177730491>.
42. Kruskal, W.H.; Wallis, W.A. Use of Ranks in One-Criterion Variance Analysis. *J. Am. Stat. Assoc.* **1952**, *47*, 583–621. <https://doi.org/10.1080/01621459.1952.10483441>.
43. Zambrano-Monserrate, M.A.; Ruano, M.A.; Yoong-Parraga, C.; Silva, C.A. Urban green spaces and housing prices in developing countries: A Two-stage quantile spatial regression analysis. *For. Policy Econ.* **2021**, *125*, 102420. <https://doi.org/10.1016/j.forpol.2021.102420>.
44. Aladwan, Z.; Ahamad, M.S.S. Hedonic Pricing Model for Real Property Valuation via GIS—A Review. *Civ. Environ. Eng. Rep.* **2019**, *29*, 34–47. <https://doi.org/10.2478/ceer-2019-0022>.
45. Hamilton, S.E.; Morgan, A. Integrating lidar, GIS and hedonic price modeling to measure amenity values in urban beach residential property markets. *Comput. Environ. Urban Syst.* **2010**, *34*, 133–141. <https://doi.org/10.1016/j.compenvurbsys.2009.10.007>.
46. Jim, C.; Chen, W.Y. Impacts of urban environmental elements on residential housing prices in Guangzhou (China). *Landsc. Urban Plan.* **2006**, *78*, 422–434. <https://doi.org/10.1016/j.landurbplan.2005.12.003>.

47. Intergovernmental Panel on Climate Change. *Climate Change 2021: The Physical Science Basis—Contribution of Working Group I to the Sixth Assessment Report of the Intergovernmental Panel on Climate Change*; Masson-Delmotte, V., Zhai, P., Pirani, A., Connors, S.L., Péan, C., Berger, S., Caud, N., Chen, Y., Goldfarb, L., Gomis, M.I., et al., Eds.; Cambridge University Press: Cambridge, UK, 2021.
48. Jedlovec, G.; Crane, D.; Quattrochi, D. Urban heat wave hazard and risk assessment. *Results Phys.* **2017**, *7*, 4294–4295. <https://doi.org/10.1016/j.rinp.2017.10.056>.
49. Morabito, M.; Crisci, A.; Gioli, B.; Gualtieri, G.; Toscano, P.; di Stefano, V.; Orlandini, S.; Gensini, G.F. Urban-Hazard Risk Analysis: Mapping of Heat-Related Risks in the Elderly in Major Italian Cities. *PLoS ONE* **2015**, *10*, e0127277. <https://doi.org/10.1371/journal.pone.0127277>.
50. Zinzi, M.; Agnoli, S.; Burattini, C.; Mattoni, B. On the thermal response of buildings under the synergic effect of heat waves and urban heat island. *Sol. Energy* **2020**, *211*, 1270–1282. <https://doi.org/10.1016/j.solener.2020.10.050>.
51. McEvoy, D.; Ahmed, I.; Mullett, J. The impact of the 2009 heat wave on Melbourne’s critical infrastructure. *Local Environ.* **2012**, *17*, 783–796. <https://doi.org/10.1080/13549839.2012.678320>.
52. Bisselink, B.; Bernhard, J.; Gelati, E.; Adamovic, M.; Guenther, S.; Mentaschi, L.; de Roo, A. *Impact of a Changing Climate, Land Use, and Water Usage on Europe’s 24 Water Resources: A Model Simulation Study*; Publications Office: Brussels, Belgium, 2018. <https://doi.org/10.2760/09027>.
53. Duran-Encalada, J.; Paucar-Caceres, A.; Bandala, E.; Wright, G. The impact of global climate change on water quantity and quality: A system dynamics approach to the US–Mexican transborder region. *Eur. J. Oper. Res.* **2017**, *256*, 567–581. <https://doi.org/10.1016/j.ejor.2016.06.016>.
54. Sulikowska, A.; Wypych, A. Seasonal Variability of Trends in Regional Hot and Warm Temperature Extremes in Europe. *Atmosphere* **2021**, *12*, 612. <https://doi.org/10.3390/atmos12050612>.
55. Hellings, A.; Rienow, A. Mapping Land Surface Temperature Developments in Functional Urban Areas across Europe. *Remote Sens.* **2021**, *13*, 2111. <https://doi.org/10.3390/rs13112111>.
56. Homaei, S.; Hamdy, M. Thermal resilient buildings: How to be quantified? A novel benchmarking framework and labelling metric. *Build. Environ.* **2021**, *201*, 108022. <https://doi.org/10.1016/j.buildenv.2021.108022>.
57. Riccioli, F.; Fratini, R.; Boncinelli, F. The Impacts in Real Estate of Landscape Values: Evidence from Tuscany (Italy). *Sustainability* **2021**, *13*, 2236. <https://doi.org/10.3390/su13042236>.
58. Kim, H.-S.; Lee, G.-E.; Lee, J.-S.; Choi, Y. Understanding the local impact of urban park plans and park typology on housing price: A case study of the Busan metropolitan region, Korea. *Landsc. Urban Plan.* **2018**, *184*, 1–11. <https://doi.org/10.1016/j.landurbplan.2018.12.007>.
59. Liebelt, V.; Bartke, S.; Schwarz, N. Hedonic pricing analysis of the influence of urban green spaces onto residential prices: The case of Leipzig, Germany. *Eur. Plan. Stud.* **2017**, *26*, 133–157. <https://doi.org/10.1080/09654313.2017.1376314>.
60. Franco, S.F.; Macdonald, J. Measurement and valuation of urban greenness: Remote sensing and hedonic applications to Lisbon, Portugal. *Reg. Sci. Urban Econ.* **2018**, *72*, 156–180. <https://doi.org/10.1016/j.regsciurbeco.2017.03.002>.
61. Czembrowski, P.; Kronenberg, J.; Czepkiewicz, M. Integrating non-monetary and monetary valuation methods—SoftGIS and hedonic pricing. *Ecol. Econ.* **2016**, *130*, 166–175. <https://doi.org/10.1016/j.ecolecon.2016.07.004>.
62. Attia, S.; Levinson, R.; Ndongo, E.; Holzer, P.; Kazanci, O.B.; Homaei, S.; Zhang, C.; Olesen, B.W.; Qi, D.; Hamdy, M.; et al. Resilient cooling of buildings to protect against heat waves and power outages: Key concepts and definition. *Energy Build.* **2021**, *239*, 110869. <https://doi.org/10.1016/j.enbuild.2021.110869>.
63. Zhang, C.; Kazanci, O.B.; Levinson, R.; Heiselberg, P.; Olesen, B.W.; Chiesa, G.; Sodagar, B.; Ai, Z.; Selkowitz, S.; Zinzi, M.; et al. Resilient cooling strategies—A critical review and qualitative assessment. *Energy Build.* **2021**, *251*, 111312. <https://doi.org/10.1016/j.enbuild.2021.111312>.
64. IEA. *IEA EBC Annex on Resilient Cooling for Residential and Small Commercial Buildings Draft Annex Text*; Annex 2018, 80; IEA: Paris, France, 2018; pp. 1–13.
65. United Nations Environment Programme. *A Practical Guide to Climate-Resilient Buildings & Communities*; UN: Nairobi, Kenya, 2021. ISBN: 978-92-807-3871-1.
66. Lin, L.; Di, L.; Zhang, C.; Guo, L.; Di, Y. Remote Sensing of Urban Poverty and Gentrification. *Remote Sens.* **2021**, *13*, 4022. <https://doi.org/10.3390/rs13204022>.
67. Hawes, J.K.; Gounaridis, D.; Newell, J.P. Does urban agriculture lead to gentrification? *Landsc. Urban Plan.* **2022**, *225*. <https://doi.org/10.1016/j.landurbplan.2022.104447>.
68. Ghosh, S.; Das, A. Modelling urban cooling island impact of green space and water bodies on surface urban heat island in a continuously developing urban area. *Model. Earth Syst. Environ.* **2018**, *4*, 501–515. <https://doi.org/10.1007/s40808-018-0456-7>.
69. Cao, J.-S.; Deng, Z.-Y.; Li, W.; Hu, Y.-D. Remote sensing inversion and spatial variation of land surface temperature over mining areas of Jixi, Heilongjiang, China. *PeerJ* **2020**, *8*, e10257. <https://doi.org/10.7717/peerj.10257>.
70. Bartesaghi-Koc, C.; Osmond, P.; Peters, A. Mapping and classifying green infrastructure typologies for climate-related studies based on remote sensing data. *Urban For. Urban Green.* **2018**, *37*, 154–167. <https://doi.org/10.1016/j.ufug.2018.11.008>.